

Arbitrary extension of the antibubble lifetime

W. Wang,^{1,2} F. Lin,³ X. Wei,⁴ J. Zou^{2,*} and S. Dorbolo⁵

¹Zhejiang University City College, Department of Mechatronics Engineering, Hangzhou 310015, China

²State Key Laboratory of Fluid Power and Mechatronic Systems,
Zhejiang University, Hangzhou 310027, China

³Ningbo Research Institute, Zhejiang University, Ningbo 315048, China

⁴Zhejiang Normal University, College of Engineering, Jinhua, 321004, China

⁵FNRS-CESAM-GRASP, Physics Department B5, University of Liège, B-4000 Liège, Belgium



(Received 24 March 2021; revised 25 September 2021; accepted 14 June 2022;
published 27 June 2022)

An antibubble is an uncommon fluid object with a unique structure: a liquid globule is wrapped by a thin air film, with the whole being immersed in a liquid bath. In short, the antibubble is the opposite of a soap bubble. The antibubble has been regarded as a promising candidate for various industrial applications since two components can be separated only by an air layer before mixing. However, the use of the antibubble is limited by the short lifetime (≈ 1 min) and the broad distribution of the lifetimes. We demonstrate a simple and efficient method to extend the lifetime of the antibubbles. The proposed system consists of a liquid surface covered by a layer of bubbles under which antibubbles are generated. The liquid is then vertically shaken. Above a given acceleration threshold that depends on the frequency, the lifetime of the antibubbles is significantly increased. Under vibrations, antibubbles were kept alive up to 13 h. As soon as the vibration is stopped, the antibubble collapses immediately. The antibubble popping can therefore be programmed. A model based on the dynamical air drainage in the air shell of the antibubble is proposed to account for these observations.

DOI: [10.1103/PhysRevFluids.7.L061601](https://doi.org/10.1103/PhysRevFluids.7.L061601)

Double emulsions are widely used in the encapsulation, delivery, and controlled release of substances since the intermediate fluid constitutes an additional barrier separating the innermost and outer fluids [1–4]. In general, the intermediate phase is an immiscible liquid with both the innermost and outer fluids. An antibubble consists in replacing the liquid in the shell with air. The result is a thin air shell separating the inner and outer liquids. This unique structure makes the antibubble a promising candidate for diverse applications [5–8]. In particular, since both liquids are separated only by an air film, we can envisage to mix or to trigger a chemical reaction on demand by popping the antibubbles. The fragile air shell makes the popping more convenient than the common liquid shell; the air may easily escape from the system. However, the short and broad distributed lifetime of antibubbles caused by the fragile air shell [9,10] constitutes the bottleneck of these envisaged techniques.

Regarding the stability of the fluid film, there exists a crucial difference between bubble and antibubble. If prevented from evaporating, a soap film can be stable for given thickness when the attracting and the repulsing forces between the interfaces balance (see, for example, Ref. [11]). Very recently, everlasting bubbles have even been discovered [12]. This is not the case for antibubbles for

*junzou@zju.edu.cn

which only attracting forces exist between the interfaces. There is no stabilization thickness for the air film. The increase of the lifetime is consequently a challenge.

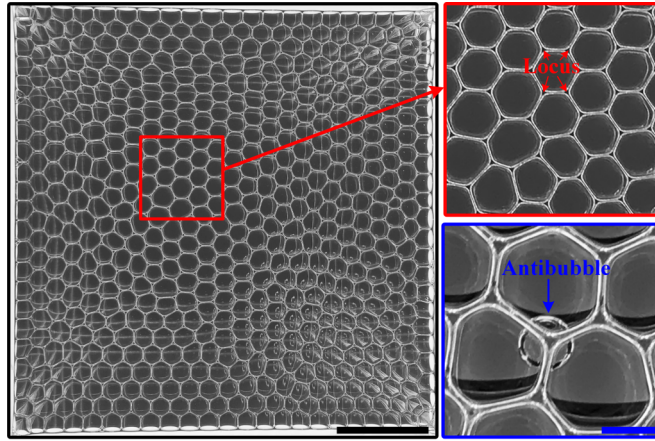
The short lifetime of antibubbles, ≈ 1 min, has been noticed since the first report in 1932 [13]. The weakness of the antibubble is the thickness of the bottom air shell. Indeed, the lifetime is governed by the slow drainage in the air shell from the bottom to the top of the antibubble under the action of the hydrostatic pressure. Consequently, the air is pushed upward while the bottom air shell thins and finally collapses when it reaches a critical thickness [9,14]. Several methods have been proposed to elongate the lifetime. Stong showed the possibility to extend the lifetime by shearing a confined antibubble in a spinning tube [15]. In this case, by entrainment of the air, the motion of the surrounding liquid allows one to homogenize the thickness of the air shell. Besides, long-lived antibubbles were generated by coating the air-liquid interfaces with hydrophobic particles [16–18]. Finally, the lifetime can be varied by changing the liquid properties, including viscosity, surface modulus, air concentration, and surfactant nature [10,19,20].

Following Stong’s experiments, increasing the lifetime by an external mechanical action should be more feasible since (i) this method does not imply the addition of particles, (ii) this can work with any kind of surfactant, and (iii) the antibubbles die when the mechanical action stops. Vertical vibrations have been proved to be an efficient method to stabilize the air film between a droplet and a liquid surface [21,22], or the liquid film between a bubble and a liquid surface [23]. Intuitively, we guess that vertical vibrations can also stabilize the antibubble by allowing the air to feed back the air film part located at the bottom of the antibubble, ensuring the existence of the air shell.

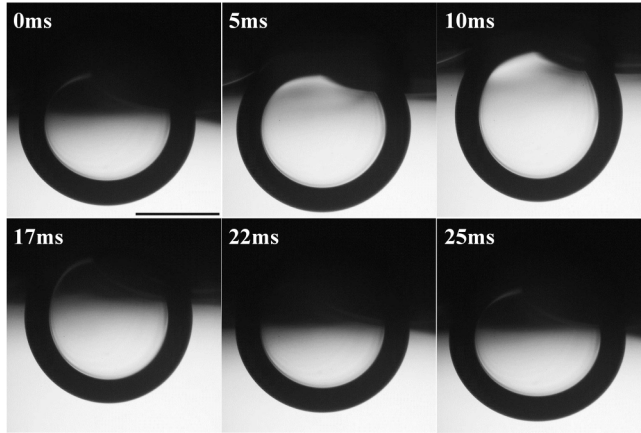
Experiments were conducted with a plexiglass container (10 cm \times 10 cm \times 15 cm) attached to an electromagnetic shaker driven by a sinusoidal signal $Y = A_m \sin 2\pi ft$, where f and A_m are the vibration frequency and amplitude, respectively. The surfactant solution in the container was a mixture of Triton X-100 solution (at 10 CMC) and glycerol with the volume ratio 2:1. Glycerol was added to increase the rate of success for the newly formed antibubbles [19]. The solution had a viscosity $\mu_l \approx 3$ mPa s and a surface tension $\sigma \approx 30$ mN/m.

Antibubbles were generated on the free surface using an intermediate soap film following the procedure described in Ref. [24]. A droplet is released above a horizontal soap film located above a liquid bath. The droplet has sufficient speed to cross the film and to become wrapped by a soapy bubble. After the collision with the liquid bath, the droplet wrapped in the bubble forms an antibubble. The vibration was then applied at 30 and 60 Hz for different amplitudes that allowed us to obtain maximum acceleration, ranging between 0 and 8 m/s². In this configuration, no significant increase of the average antibubble lifetime was observed; even worse, the lifetime decreased at high accelerations (see the Supplemental Material, Sec. 1 [25]). Actually, the Faraday waves [26] were rapidly generated at the surface of the liquid bath, which harms the antibubble stability because of the severe perturbations. Moreover, we note that the Faraday waves led to the “walking antibubble” [27], which collapsed immediately as it touched the container walls (see Movie 1 [25]).

To reduce the Faraday waves, the liquid surface was covered by a layer of bubbles (see also the Supplemental Material, Sec. 2). Such a layer allows a large energy dissipation and significantly increases the Faraday threshold [28]. The bubble layer was produced by injecting air with a bent stainless needle and the bubble diameter d was adjusted by changing the air flow speed in the tube. In Fig. 1(a), we show the top view of the bubble layer. In fact, the bubble layer cannot only reduce the Faraday waves but also results in two advantages. First, it provides a convenient way for generating antibubbles, as described in Ref. [29]. Antibubbles can be generated by releasing droplets directly on the bubble layer, which plays the role of the soap film to assist the antibubble formation. Second, the layer allows us to localize the antibubbles and to avoid any lateral motion. Indeed, between three neighboring bubbles, a locus for one antibubble is formed whose apex is constituted by a plateau border. During the vibrations, the antibubble moved up and down in one of the loci, as shown in Fig. 1(b). After the vertical vibration was switched on, we found that some antibubbles could exist for a much longer time when the vibrations were strong enough. The maximum lifetime observed was about 13 h.



(a)



(b)

FIG. 1. (a) Top view of the foam layer. Three neighboring bubbles form a locus and the generated antibubble is trapped in it to avoid any lateral motion. The black scale bar indicates 20 mm while the blue one indicates 2 mm. (b) Dynamics of an antibubble under vertical vibration ($f = 40$ Hz, $A_m = 0.067$ mm). It maintains a spherical shape during vibration. The scale bar indicates 1 mm.

Systematic experiments were then conducted to measure the effect of vertical vibrations on the antibubble lifetime. At a fixed frequency, we increased the amplitude step by step. For each step, more than 50 antibubbles were produced and the lifetimes τ were measured using a high-speed camera. The cumulative distribution function (CDF) of the antibubble lifetimes are presented in Fig. 2 under different vibration conditions. The experimental CDF were fitted using the Weibull statistical model F

$$F(\tau) = 1 - \exp[-(\tau/\lambda)^k], \quad (1)$$

where λ and k are the scale and shape factor, respectively. The values of λ and k are reported in Table I for both considered excitation frequencies and for the different accelerations of the vibration.

The variation of the statistical expectation E given by $E = \lambda\Gamma(1 + 1/k)$ is presented in Fig. 2(c). We can see that E sharply increases between $a_m = 4.94$ m/s² and 6.27 m/s² for $f = 30$ Hz and between $a_m = 6.09$ m/s² and 7.55 m/s² for $f = 60$ Hz. This behavior suggests the existence of a threshold for the acceleration above which the antibubble lifetime is significantly increased. Second,

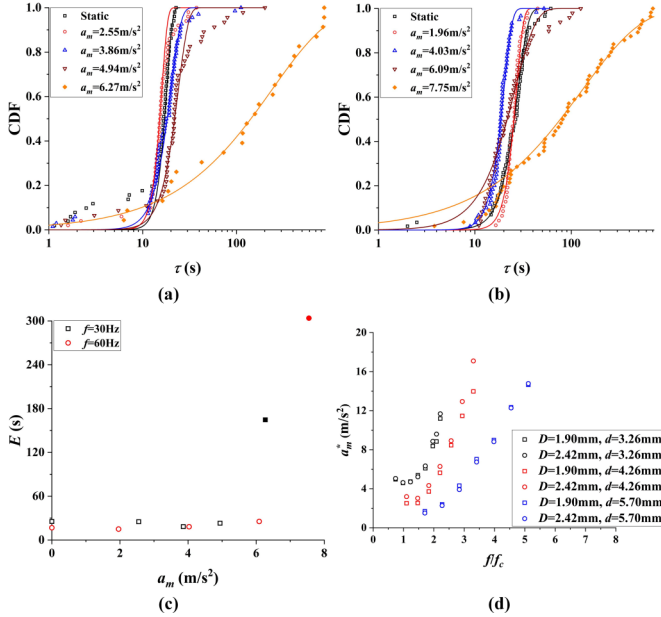


FIG. 2. [(a), (b)] CDF of the antibubble lifetime varying with the vibration acceleration for $f = 30$ Hz and $f = 60$ Hz, respectively. The solid lines are fitted with the Weibull statistical model. (c) Variation of the statistical expectation of the antibubble lifetime, E , with the vibration acceleration. The solid symbols in (a), (b), and (c) indicate that at least one antibubble survives 900 s; otherwise, it is a hollow symbol. (d) Variation of the threshold acceleration for the long-lived antibubbles with the vibration frequency.

the shape factor k decreases from a value larger than 1 to a value $k < 1$ in the same range of accelerations as observed for E . Note that when $k > 1$ the popping probability increases with time and the mechanism of popping is then interpreted as an aging process caused by the air drainage. On the other hand, when $k < 1$ the popping probability decreases due to the external vibrations. This suggests the popping mechanism changes when the vibration acceleration is above a given threshold a_m^* that depends on the frequency.

In practice, we have used another procedure to obtain the threshold acceleration based on the CDF's analysis for the save of experimental time. Indeed, the transition was found to be rather

TABLE I. Fitting parameters of the experimental cumulate distribution function of the lifetimes obtained for four different accelerations and two different frequencies. The fit curves are presented in Figs. 2(a) and 2(b).

f (Hz)	a_m (m/s^2)	λ (s)	k
30	0	18	7
	2.55	16	7
	3.86	20	4
	4.94	24	4
	6.27	240	0.7
60	0	28	4
	1.96	27	6
	4.03	20	5
	6.09	26	2
	7.55	130	0.7

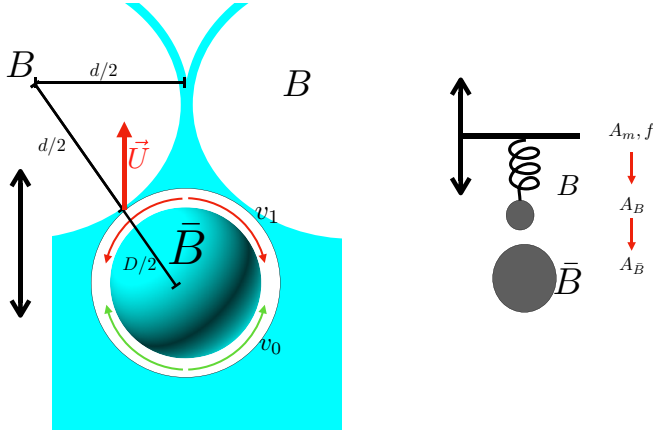


FIG. 3. Sketch of the vibrating antibubbles under a foam layer. The symbols B and \bar{B} indicate the bubble and antibubble, respectively. On the right, the mechanical model of the system is presented. The foam layer is modeled by a spring and the antibubble as a mass that is attached to the spring. The vibration of the plate (A_m, f) induces the vibration of the spring-mass (the bubbles) with an amplitude A_B , which in turn produces the motion of the antibubble with an amplitude $A_{\bar{B}}$.

steep. We defined a long-lived antibubble as an antibubble that lasts at least more than $\tau^* = 900$ s. We claim that the considered acceleration is above the acceleration threshold a_m^* if at least two antibubbles out of 50 can survive 900 s. Regarding the Weibull CDF, our criterion writes $F(\tau^*) < 0.96$; for $k = 1$, that represents a statistical expectation of about 280 s, which is about 15 times the statistical expectation of the lifetime at rest. To be clear, the emergence of the long-lived antibubbles does not mean all the antibubbles can survive 900 s. However, the proportion of the long-lived antibubbles increases with the acceleration. When the acceleration is high enough, almost all the generated antibubbles can survive 900 s (see Movie 2 [25]).

The variation of the threshold acceleration with the dimensionless frequency $r = f/f_c$ is reported in Fig. 2(d), where the characteristic frequency (capillary frequency) is given by $f_c = \sqrt{\sigma/\rho_l d^3}$, where $\rho_l = 1000 \text{ kg/m}^3$ is the density of the surfactant mixture. We observe that the antibubble diameter D has a weak influence on the acceleration threshold while the bubble diameter d plays a dominant role. For $d = 3.26$ and 4.26 mm, a minimum can be observed at $r \approx 1$, which suggests the signature of a resonance process induced by the bubbles. Moreover, no long-lived antibubbles can be observed at the lower frequency, even when the acceleration was much higher than the present value. The threshold acceleration for $d = 5.70$ mm increases monotonically with the frequency since the the minimum frequency studied is larger than the corresponding critical frequency.

A theoretical model is needed to elucidate the critical conditions for the long-lived antibubbles. In Ref. [9], for an antibubble at rest, the air in the film is drained upward under the action of the hydrostatic pressure $\Delta P = \rho g D$, as shown in Fig. 3 (green arrows). The air speed v_0 is related to the hydrostatic pressure and the air film thickness ε_0 through the lubrication equation

$$\frac{2\Delta P}{\pi D} = \mu_a \frac{v_0}{\varepsilon_0^2}, \quad (2)$$

where ε_0 is the averaged thickness of the air shell and μ_a is the air viscosity. One can obtain a scaling for the lifetime τ by dividing the half of the antibubble perimeter by the speed, $\tau \sim \mu_a D / \rho g \varepsilon_0^2$. A much more complete and precise study can be found in Refs. [10,30]. In order to increase the lifetime, the air speed v_0 should be decreased or, even better, reversed. One can think about a change of gravity (a perspective should be 0 g) or the rapid rotation of the whole system as suggested by Stong [15] to entrain the air from the top to the bottom of the antibubble. In the present conditions,

as shown in Fig. 3(a), the antibubble comes in contact with the foam layer, and the foam provides a vertical speed U to the antibubble equals to $2\pi A_{\bar{B}}f$, where $A_{\bar{B}}$ is the antibubble vibration amplitude. The antibubble is submitted to a dynamical pressure $\frac{1}{2}\rho U_d^2$, where U_d is the component of the speed directed toward the center of the antibubble [31]. We have the following geometrical relation

$$U_d = \phi(d, D)U.$$

The value of ϕ is given by $\phi = \sqrt{(D^2 + 2Dd)/(d + D)}$.

We can estimate the speed resulting from the pressure pulse

$$\frac{\frac{1}{2}\rho U_d^2}{\ell} = \mu_a \frac{v_1}{\varepsilon_0^2}, \quad (3)$$

where v_1 is the air speed oriented from the north pole toward the south one (the red arrows), and ℓ is the distance on which the pressure gradient is exerted. This distance ℓ is assumed to be proportional to the distance between the contact points of the antibubble and the bubbles; here, we took $\ell = \pi D/2$. The critical condition for an immortal antibubble is $v_1 \simeq v_0$, which implies for U

$$U^2 = \frac{4}{\pi\phi^2}g\ell. \quad (4)$$

This means that the maximum speed of the antibubble should be larger than a constant $\phi^{-1}\sqrt{\frac{4}{\pi}g\ell}$, which depends on the geometric relation between the antibubble and the foam layer.

The speed U is related to the forced vibration through the following chain. The forced vibration (A_m, f) induces the oscillation of the bubble layer with an amplitude A_B and the same frequency f (see Movie 3 [25]). In turn, the energy is transmitted to the antibubble, which periodically bounces on the surface bubbles with an amplitude $A_{\bar{B}}$ and a frequency f . The relation between the two amplitudes is $A_{\bar{B}} = \beta(D, d)A_B$, where $\beta(D, d)$ depends on geometric relation between the antibubble size D and the bubble size d .

We model the bubble as a spring-mass system, with the elastic coefficient $\sim\sigma$ and mass $m \sim \rho_l d^3$. We consider that the antibubble is nondeformable compared to the bubbles due to the double interface and the viscosity of the liquid surrounding and inside the antibubble that damps the oscillations. As shown in Fig. 2(b), the antibubble remains spherical during vibrations. The bubble has a natural frequency $f_0 = \alpha f_c = \alpha\sqrt{\sigma/\rho_l d^3}$, where α is a constant. Under vertical vibrations, we obtain the bubble motion equation

$$m\ddot{x} + c\dot{x} + kx = 2\pi c f A_m \cos 2\pi f t + k A_m \sin 2\pi f t, \quad (5)$$

where x indicates the mass center of the liquid displaced by the bubble and c is the damping coefficient. The two terms of the right side indicate the damping force caused by the surrounding liquid and the elastic force by surface tension, respectively. With the amplitude ratio $\lambda = A_{\bar{B}}/A_m$ and the reduced frequency $r = f/f_c$, we obtain

$$\lambda \sim \frac{\alpha\sqrt{\alpha^2 + 4v^2 r^2}}{\sqrt{(\alpha^2 - r^2)^2 + 4v^2 \alpha^2 r^2}}, \quad (6)$$

where $v = c/2\sqrt{km}$ is the damping ratio. To challenge this model, we measured the oscillation amplitude $A_{\bar{B}}$ of the bubble bottom for the three considered bubble diameters, $d = 3.26, 4.26,$ and 5.70 mm. The value λ/r^2 , indicating the acceleration ratio between the bubble and the platform, is represented as a function of the parameter r in Fig. 4. In so doing, the data collapse on one single curve that can be fitted with Eq. (6), the purple line ($\alpha^2 = 2.7$ and $v^2 = 0.005$) in Fig. 4. On the other hand, large deviations can be observed, especially at large frequencies, since the theoretical model actually indicates the motion of the bubble mass center rather than the bottom boundary.

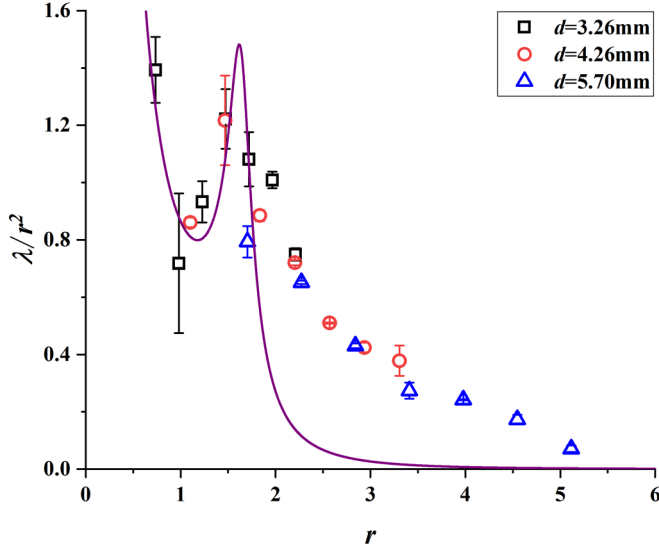


FIG. 4. The amplitude ratio $\lambda = A_B/A_m$ divided by r^2 is plotted as a function of r for the three considered bubble diameters (see legend). The purple line is fitted with Eq. (6).

In consequence, we can model the long-lived threshold with respect to the vibration parameters (A_m, f). The long lifetime is guaranteed when

$$U = 2\pi A_B f = 2\pi \beta A_B f = 2\pi \beta A_m f \lambda > \frac{2}{\phi} \sqrt{g\ell/\pi}.$$

Finally, we obtain the scaling for threshold of a long-living antibubble

$$2\pi f A_m^* = \frac{\xi}{\beta} \frac{\sqrt{2gD}}{\phi} \frac{1}{\lambda}. \quad (7)$$

The basic model predicts a threshold that can be only but larger than the experimental threshold because the manner to experimentally determine the threshold depends on an arbitrary lifetime (900 s). The parameter ξ is a multiplicative factor that accounts for the fact that the experimental determination of the threshold underestimates the theoretical threshold because of our 900-s criterion.

In Fig. 5(a), we report $2\pi f A_m^*$ as a function of $r = f/f_c$. The immortal threshold is minimum when $r \simeq 1.5$. The experimental results are fitted with $\alpha^2 = 2.7$ but $\nu^2 = 0.2$ (they are the continuous lines in the figure). This larger damping ratio can be attributed to the presence of the antibubbles.

The multiplicative parameter ξ and the energy transmission from the bubble to the antibubbles β are unknown. In Fig. 5(b), the found values of ξ/β , obtained thanks to the fit of Eq. (6), are reported as a function of the bubble diameters. For each value of d , two values of ξ/β are obtained that correspond to the antibubble diameters $D = 1.90$ and $D = 2.42$ mm, respectively. The ratio ξ/β is found to be more influenced by the bubble size than by the antibubble size. The geometrical factor embedded in the factor β is not modeled here. The determination of the precise dependence of the sizes of the antibubble and of the bubbles on the energy transmission requires a fine understanding of the coupling between the deformation of the bubbles and of the antibubble. Experimentally speaking, this requires us to capture the deformation of the bubbles and of the antibubble in parallel with the fluid motion surrounding the antibubble.

In summary, we demonstrate a simple and efficient method to extend and control the lifetime of antibubbles. The surface bubbles suppress the Faraday waves, allow us to localize the

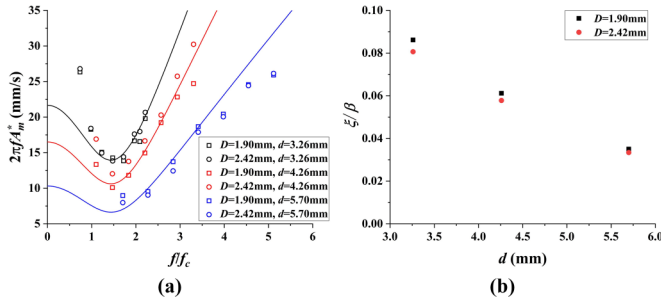


FIG. 5. (a) The threshold maximum speed $2\pi f A_m^*$ as a function of the reduced frequency for the six combinations of antbubbles and bubbles. The curves correspond to the model Eq. (6). (b) Values of ξ/β obtained by fitting Eq. (6) as a function of the bubble diameter d .

antbubbles thanks to the deformation of the interface, and act as a resonator to drive the motion of the antbubbles. Then, the vertical vibrations inhibit the unidirectional air flow in the air film and stabilize the antbubbles. A theoretical model was proposed to elucidate the threshold for a long-living antbubble. Moreover, the foam-coated system should worth future attention since the locus formed by the neighboring bubbles allows the direct manipulation on a single fluid particle, which is significant in microfluidics manipulation.

Authors acknowledge the support from the NSFC (Grants No. 51875507 and No. U1908228). S.D. thanks F.R.S.-FNRS for financial support and also Prof. N. Vandewalle for the use of the GRASP facilities. The authors also thank B. Scheid (ULB, Belgium) for fruitful discussion about the interplay between the drainage and the oscillation regime.

-
- [1] A. S. Utada, E. Lorenceau, D. R. Link, P. D. Kaplan, H. A. Stone, and D. A. Weitz, Monodisperse double emulsions generated from a microcapillary device, *Science* **308**, 537 (2005).
 - [2] A. G. Marin, I. G. Loscertales, M. Marquez, and A. Barrero, Simple and Double Emulsions Via Coaxial Jet Electrosprays, *Phys. Rev. Lett.* **98**, 014502 (2007).
 - [3] N. Pannacci, H. Bruus, D. Bartolo, I. Etchart, T. Lockhart, Y. Hennequin, H. Willaime, and P. Tabeling, Equilibrium and Nonequilibrium States in Microfluidic Double Emulsions, *Phys. Rev. Lett.* **101**, 164502 (2008).
 - [4] J. Zhang, R. J. Coulston, S. T. Jones, J. Geng, O. A. Scherman, and C. Abell, One-step fabrication of supramolecular microcapsules from microfluidic droplets, *Science* **335**, 690 (2012).
 - [5] W. Suhr, Gaining insight into antbubbles via frustrated total internal reflection, *Eur. J. Phys.* **33**, 443 (2012).
 - [6] J. E. Silpe and D. W. McGrail, Magnetic antbubbles: Formation and control of magnetic macroemulsions for fluid transport applications, *J. Appl. Phys.* **113**, 17B304 (2013).
 - [7] S. Kotopoulos, K. Johansen, O. Gilja, A. Poortinga, and M. Postema, Harmonic response from microscopic antbubbles, *Acta Phys. Pol. A* **127**, 99 (2015).
 - [8] M. Postema, A. Novell, C. Sennoga, A. T. Poortinga, and A. Bouaka, Harmonic response from microscopic antbubbles, *Appl. Acoust.* **137**, 148 (2018).
 - [9] S. Dorbolo, E. Reyssat, N. Vandewalle, and D. Quere, Aging of an antbubble, *EPL* **69**, 966 (2005).
 - [10] Y. Vitry, S. Dorbolo, J. Vermant, and B. Scheid, Controlling the lifetime of antbubbles, *Adv. Colloid Interface Sci.* **270**, 73 (2019).
 - [11] J. Israelachvili, Direct measurements of forces between surfaces in liquids at the molecular level, *Proc. Natl. Acad. Sci. USA* **84**, 4722 (1987).

- [12] A. Roux, A. Duchesne, and M. Bauduin, Everlasting bubbles and liquid films resisting drainage, evaporation, and nuclei-induced bursting, *Phys. Rev. Fluids* **7**, L011601 (2022).
- [13] W. Hughes and A. R. Hughes, Liquid drops on the same liquid surface, *Nature (London)* **129**, 59 (1932).
- [14] P. G. Kim and H. A. Stone, Dynamics of the formation of antibubbles, *EPL* **83**, 54001 (2008).
- [15] C. L. Stong, Curious bubbles in which a gas encloses a liquid instead of the other way around, *Sci. Am.* **230**, 116 (1974).
- [16] A. T. Poortinga, Long-lived antibubbles: Stable antibubbles through Pickering stabilization, *Langmuir* **27**, 2138 (2011).
- [17] J. E. Silpe, J. K. Nunes, A. T. Poortinga, and H. A. Stone, Generation of antibubbles from core-shell double emulsion templates produced by microfluidics, *Langmuir* **29**, 8782 (2013).
- [18] A. T. Poortinga, Micron-sized antibubbles with tunable stability, *Colloids Surf. A* **419**, 15 (2013).
- [19] S. Dorbolo, D. Terwagne, R. Delhalle, J. Dujardin, N. Huet, N. Vandewalle, and N. Denkov, Antibubble lifetime: Influence of the bulk viscosity and of the surface modulus of the mixture, *Colloids Surf. A* **365**, 43 (2010).
- [20] B. Scheid, J. Zawala, and S. Dorbolo, Gas dissolution in antibubble dynamics, *Soft Matter* **10**, 7096 (2014).
- [21] Y. Couder, E. Fort, C.-H. Gautier, and A. Boudaoud, From Bouncing to Floating: Noncoalescence of Drops on a Fluid Bath, *Phys. Rev. Lett.* **94**, 177801 (2005).
- [22] T. Gilet, D. Terwagne, N. Vandewalle, and S. Dorbolo, Dynamics of a Bouncing Droplet onto a Vertically Vibrated Interface, *Phys. Rev. Lett.* **100**, 167802 (2008).
- [23] J. Zawala, S. Dorbolo, D. Terwagne, N. Vandewalle, and K. Malysa, Bouncing bubble on a liquid/gas interface resting or vibrating, *Soft Matter* **7**, 6719 (2011).
- [24] J. Zou, W. Wang, C. Ji, and M. Pan, Droplets passing through a soap film, *Phys. Fluids* **29**, 062110 (2017).
- [25] See Supplemental Material at <http://link.aps.org/supplemental/10.1103/PhysRevFluids.7.L061601> for the average antibubble lifetime and movie descriptions.
- [26] M. Faraday, On a peculiar class of acoustical figures; and on certain forms assumed by groups of particles upon vibrating elastic surfaces, *Philos. Trans. R. Soc. London* **121**, 299 (1831).
- [27] Y. Couder, S. Protiere, E. Fort, and A. Boudaoud, Walking and orbiting droplets, *Nature (London)* **437**, 208 (2005).
- [28] A. Bronfort and H. Caps, Faraday instability at foam-water interface, *Phys. Rev. E* **86**, 066313 (2012).
- [29] L. Bai, W. Xu, P. Wu, W. Lin, C. Li, and D. Xu, Formation of antibubbles and multilayer antibubbles, *Colloids Surf. A* **509**, 334 (2016).
- [30] B. Scheid, S. Dorbolo, L. R. Arriaga, and E. Rio, Antibubble Dynamics: The Drainage of an Air Film with Viscous Interfaces, *Phys. Rev. Lett.* **109**, 264502 (2012).
- [31] C. Wang and M. Gharib, Physics of a strongly oscillating axisymmetric air-water interface with a fixed boundary condition, *Phys. Rev. Fluids* **7**, 044003 (2022).